CHEMPHYSCHEM

DOI: 10.1002/cphc.200600186

Adsorption and Dynamics of Long-Range Interacting Fullerenes in a Flexible, Two-Dimensional, Nanoporous Porphyrin Network

Andreas Kiebele,[a] Davide Bonifazi,[b] Fuyong Cheng,[b] Meike Stöhr,[a] François Diederich,[b] Thomas Jung,[c] and Hannes Spillmann*[a]

Herein, a detailed investigation of the adsorption and dynamics of C_{60} and C_{70} fullerenes hosted in a self-assembled, two-dimensional, nanoporous porphyrin network on a solid Ag surface is presented. Time-resolved scanning tunneling microscopy (STM) studies of these supramolecular systems at the molecular scale reveal distinct host–guest interactions giving rise to a pronounced dissimilar mobility of the two fullerenes within the porphyrin network. Furthermore, long-range coverage-dependent interactions between the all-carbon guests, which clearly affect their mobility and are likely mediated by a complex mechanism involving the Ag substrate and the flexible porphyrin host network, are observed. At increased fullerene coverage, this unprecedented interplay results in the formation of large fullerene chains and islands. By applying a lattice gas model with nearest-neighbor interactions and by evaluating the fullerene-pair distribution functions, the respective coverage-dependent guest–guest interaction energies are estimated.

1. Introduction

Recently, there has been an increasing interest in the synthesis of rationally designed nanoporous molecular materials for a large variety of applications, such as gas sorption, catalysis, shape-selective recognition, and chemical sensing.[1–6] Although thermally less stable than traditional inorganic zeolites, such "soft" porous materials feature an enormous chemical and structural versatility, because they are built by bottom-up linkage of easily modifiable molecular building blocks. Today, examples of multifunctional, flexible, and dynamic organic and metal-organic frameworks, which respond to external stimuli such as light, electric fields, or the presence of guest molecules by adapting their pores and corresponding physicochemical properties reversibly, are known.[7–12]

Lately, two-dimensional (2D) inorganic, organic, and metal-organic porous analogues have been successfully formed on solid surfaces using a similar bottom-up approach. Several frameworks capable of hosting guest molecules have been reported, and host–guest interactions have been investigated, for example, by temperature-controlled desorption studies of the accommodated guest molecules, or by electron spectroscopy.[13–20] For the well-established three-dimensional (3D) zeolites, it has been recognized, however, that diffusive transport of the guest molecules within the porous matrix, together with host–guest and guest–guest interactions, play a crucial role when the frameworks are supposed to act as catalysts or as supports for surface chemical reactions. Consequently, diffusion of the molecular guests within the host has been studied as a function of temperature, chemical structure, and the fractional loading of the zeolites, in numerous experimental and theoretical studies.[21–29] However, in surface-supported 2D porous frameworks, to our knowledge, no data addressing lateral interguest interactions or guest mobility, are available.

Herein, we present the first comprehensive study of a 2D porous porphyrin network on an Ag surface capable of hosting C_{60} and C_{70} fullerene guest molecules. In this unique network, the weak physisorptive host–guest interactions allow single fullerene molecules to displace themselves to neighboring pores by thermal activation at 298 K. Time-lapse imaging experiments conducted with a scanning tunneling microscope (STM) allowed a systematic investigation of the mobility of the hosted species as a function of the loading and chemical structure of the guest molecules on the molecular scale. Interpretation of these data within a quasichemical approach, which describes a 2D lattice gas with interacting particles, reveals long-

[a] *A. Kiebele, Dr. M. Stöhr, Dr. H. Spillmann*
NCCR Nanoscale Science, Department of Physics, University of Basel
Klingelbergstrasse 82, 4056 Basel, (Switzerland)
Fax: (+41) 061-267-3784
E-mail: h.spillmann@unibas.ch

[b] *Dr. D. Bonifazi, Dr. F. Cheng, Prof. Dr. F. Diederich*
Organic Chemistry Laboratory, ETH-Hönggerberg, HCI
8093 Zürich (Switzerland)

[c] *Dr. T. Jung*
Laboratory for Micro- and Nanotechnology
Paul Scherrer Institute, 5232 Villigen PSI (Switzerland)

Supporting information for this article is available on the WWW under http://www.chemphyschem.org or from the author.

range, complex interguest interactions that are effective over distances much longer than van der Waals radii.

2. Results and Discussion

Deposition of 0.5–0.7 monolayers (ML) of porphyrin **1** (Figure 1 a) on Ag(111) results in the self-assembly of a supramolecular network featuring hexagonally arranged pores with a pore–pore distance of 3.3 ± 0.1 nm (Figures 1 b and c).

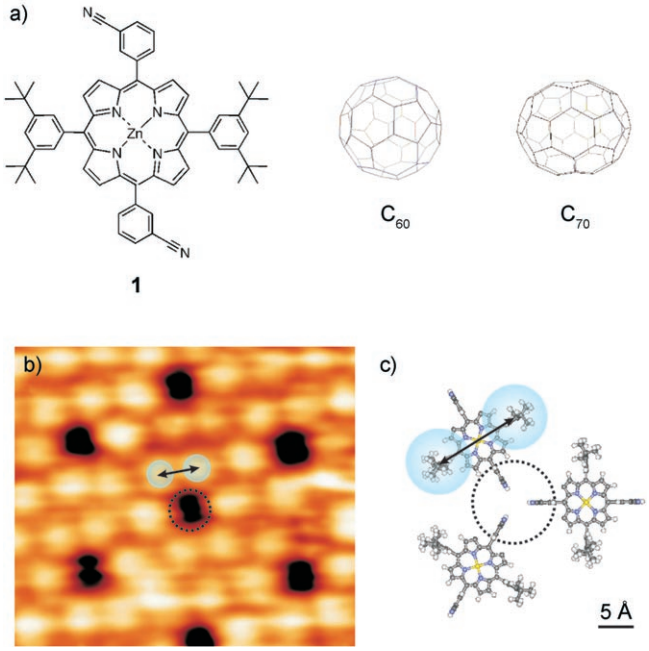

Figure 1. a) Chemical structures of the molecules used in this study. For comparison, the structures are drawn to scale. b) Porphyrin derivative **1**[61] self-assembles in an hexagonal porous host network on Ag(111), as shown in the STM image (scan range: 9.1 × 8.0 nm^2, sample bias voltage, V_{bias} = 2.9 V, tunneling current, I_t = 25 pA, T = 298 K). As previously reported, single porphyrin **1** appeared as two bright protrusions (3,5-di(*tert*-butyl)-phenyl substituents), which are separated by about 1.2 nm (double arrow).[30] c) According to the proposed model, each pore consists of three concentrically arranged porphyrin molecules. All 3,5-di(*tert*-butyl)phenyl moieties and the 3-cyanophenyl substituents are drawn perpendicular with respect to the central porphyrin macrocycle for reasons of clarity. However, the real conformation is likely to be different as deduced from the slightly different distances and brightness of the protrusions in the STM image (b).

Upon subsequent sublimation of C_{60}, single fullerene molecules adsorb into these pores as reported earlier.[30] It has been noted that the C_{60} molecules show a disposition for lateral displacement, due to thermal activation at 298 K. In order to investigate this movement in more detail, it has been found meaningful to vary not only the guest molecule coverage, but moreover to exchange the molecules hosted in the pores. For this reason, C_{70} molecules were evaporated onto the same hexagonal porphyrin network for comparison.

2.1. Adsorption of C_{60} and C_{70} in the Host Network

At first glance, the STM images of C_{70} and C_{60} on the porous porphyrin lattice seem very similar (Figures 2 a and d).

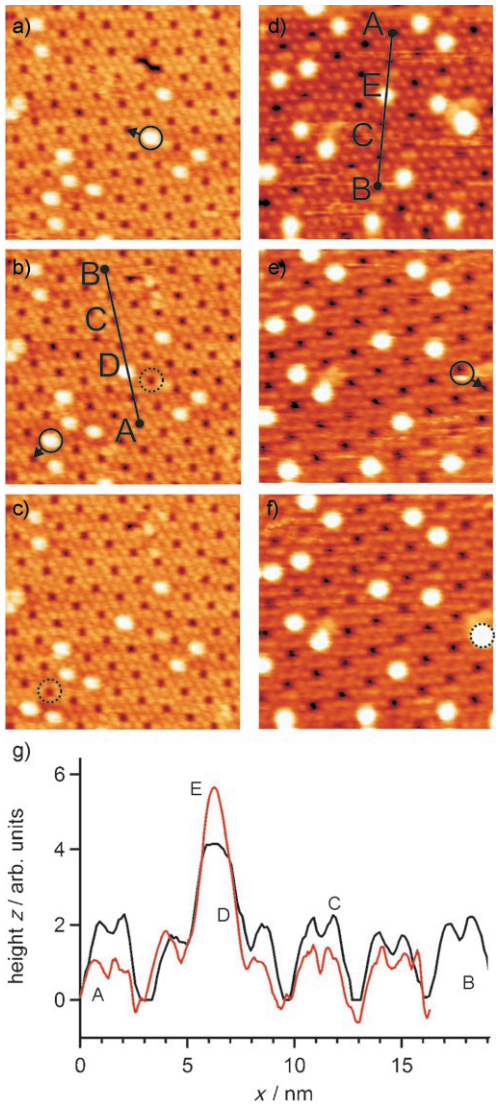

Figure 2. a–c) Series of consecutive STM images of C_{60} (labeled D) molecules on the porous porphyrin network (scan range: 30 × 30 nm^2, V_{bias} = 2.9 V, I_t = 12 pA, T = 298 K). The time lapse between two measurements is 62 s. d–f) Series of consecutive STM images of C_{70} (labeled E) molecules on the porous porphyrin network (scan range: 25 × 25 nm^2, V_{bias} = 2.0 V, I_t = 12 pA, T = 298 K). The time lapse between two measurements is 89 s. ○: molecules that have moved between subsequent pictures, dashed circles indicate former positions of molecules. g) Line sections of the porphyrin network (labeled C) with C_{60} (black) and C_{70} (red) from measured data along the black lines from A to B.

Both guest molecules adsorb concentrically into the pores of the underlying network and appear as bright protrusions with an indistinguishable lateral diameter of 1.7 ± 0.3 nm (full width at half maximum), as exemplarily shown by the line sections in Figure 2 g. Note that, owing to the finite size of the STM tip, the lateral dimensions of single molecules are broadened by the tip–surface convolution. In contrast to the work of Katsonis et al., who found C_{70} molecules with an elliptical shape at an Au(111) surface,[31] the fullerenes on the porphyrin network always appear with spherical symmetry. As well, no submolecular structure of the C_{70} spheres could be observed, as opposed to the intermixed C_{60}/C_{70} monolayer on Cu(111) re-

ported by Wang et al.[32] This difference may be caused by the relatively weak adsorption energy of the fullerenes in the present porphyrin framework compared to the stronger metal–fullerene interaction in the above-mentioned reports, which forces the C_{70} molecules to adsorb steadily with the long side parallel to the surface. This indicates that the fullerenes in the pores of the supramolecular assembly of **1** are able to vibrate and rotate at 298 K, which is confirmed by their averaged round appearance on the time scale of STM measurements.

However, it is expected that C_{60} and C_{70} can be discriminated by their different apparent heights in STM.[31,32] For a meaningful analysis, the apparent height measurements need to be normalized before they can be compared, in order to account for different STM tip geometries. It has been shown[33,34] that this can be achieved by normalizing the height histogram of two different measurements with a characteristic peak, corresponding to a common substructure in the two STM images. In the present study, the apparent height of the pure porphyrin network provides a suitable point of reference, since it very likely shows a constant corrugation, independent of the presence of guest molecules. Figure 3 shows histograms of apparent heights of three representative STM images.

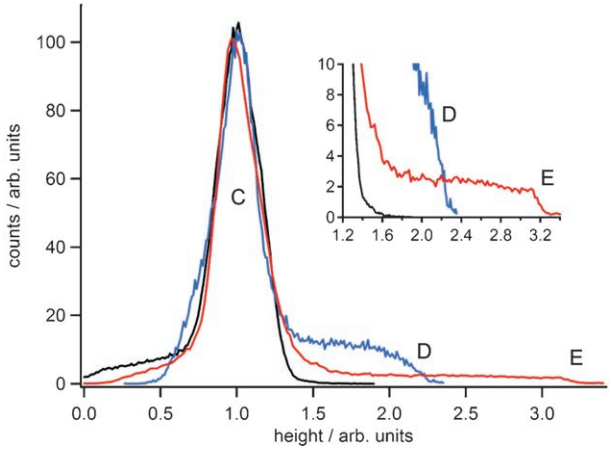

Figure 3. a) Normalized histograms of the distribution of apparent heights for a clean porphyrin network (black), a porphyrin network with C_{60} (blue), and one with C_{70} (red). The inset shows the cutoff positions of C_{60} and C_{70} (labeled D and E) in detail.

The curves have been normalized by adjusting the position, width, and height of the dominant peak (labeled C), representing the porphyrin layer. In the detailed view (inset of Figure 3), one can clearly see that the normalized curves of C_{60} (blue) and C_{70} (red) feature distinctly different cutoff positions, as indicated by labels D and E, respectively. These characteristic features—which are completely absent when no guest molecules are present (black)—reflect the maximum height in each STM image, and are caused by the fullerene guests. Applying this method, the ratio of the measured height of C_{70} [$h_a(C_{70})$] to that of C_{60} [$h_a(C_{60})$] was calculated to $h_a(C_{70})/h_a(C_{60}) = 1.5 \pm 0.1$. This result was found to be independent of the quality of the STM images caused by different tip geometries and the guest molecule coverage. Scan parameters, such as bias voltage, scan size, or scan speed also did not affect the height ratio.

The value of ≈ 1.5 for the measured height ratio deviates significantly from the maximum ratio of ≈ 1.13, which was obtained by pure geometrical consideration of the van der Waals diameter of the two fullerenes [$d(C_{60}) \approx 10.6$ Å,[35,36] $d_{max}(C_{70}) \approx 12.0$ Å[37,38] (see also the Experimental Section)]. A similar observation has been reported for a co-deposited C_{60} and C_{70} monolayer on an Au(111) where the height ratio $h_a(C_{70})/h_a(C_{60})$ was determined as 1.4 ± 0.2 from an analysis of STM cross-sections.[31] Since topographic differences can be excluded when both fullerenes are in direct contact with the metal substrate, the increased height ratio can be purely attributed to different electronic metal–fullerene coupling. For the fullerenes adsorbed within the porphyrin-based pores, the situation is even more complicated. On the one hand, the different electronic properties of C_{70} compared to those of C_{60} (e.g. electron affinity, ionization potential, or highest occupied molecular orbital–lowest unoccupied molecular orbital, HOMO–LUMO, gap[39]) are expected to result in unequal host–guest interactions. On the other hand, the oblong shape of C_{70} compared to the spherical shape of C_{60} likely demands a different adsorption geometry in the pores, either by standing upright, lying on the long side (thus not fitting as far down the pore), or some (dynamic) variation of the two. Overall, the measured height ratio is indicative of a dissimilar interaction with the pores, and therefore the host–guest interaction energies for the two fullerene molecules are expected to be different.

2.2. Mobility of Single Fullerene Molecules

In order to investigate the mobility of the guest molecules, time-lapse imaging experiments were performed as shown in Figure 2 a-f (see also Movies 1 and 2 in the Supporting Information). In both series, individual fullerenes (C_{60} and C_{70}) were found to move from one pore to a neighboring one by thermal activation at 298 K. On the timescale of one STM measurement (from one to a few minutes), only some molecules move, while most stay at their adsorption site. This singles out STM as an adequate technique for examining the dynamics of these fluctuating supramolecular structures. In order to minimize the potential influence of the scanning on the hopping process, all images were recorded using a large tunneling-gap resistance of more than 100 GΩ.

By analyzing the positions of a large number of molecules over several consecutive STM images, one can determine the respective displacements and their relative occurrence in dependence of the elapsed time. Practically, the position of 200–1000 fullerene molecules (number depending on the available STM data) were observed and analyzed in displacement histograms, as exemplarily shown for C_{60} in Figure 4 b.

The peaks in the histogram, which are centered around the discrete distances of a hexagonal porous lattice as depicted in Figure 4 a, clearly show that the guest molecules move by means of a hopping process from pore to pore. This finding is a consequence of the fact that the guest molecules are re-

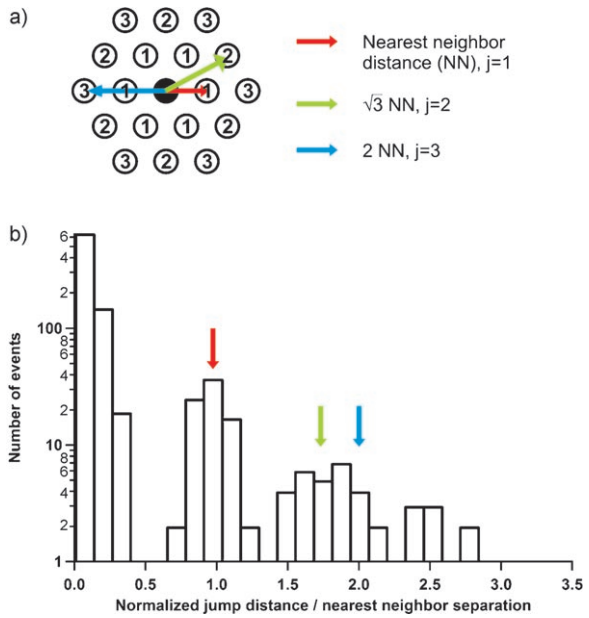

Figure 4. a) Schematic representation of the 2D porous hexagonal network. The numbers indicate the index *j* of the distance between the center and the respective neighboring site. The colored arrows indicate the nearest (NN, red), next nearest ($\sqrt{3}$NN, green), and second nearest neighbor (2NN, blue) distances. b) Example of a histogram of jump distances of C_{60} on the porous porphyrin network. The position of 939 guest molecules in an STM movie (scan range: 100×100 nm^2, scan speed: 144 s per frame, 14 frames) was analyzed over a total time period of 33 min. Note the distinct peaks at 1, 1.73, and 2 nearest neighbor distances. The spreading of the peaks was caused by the inhomogeneous drift during scanning, which alters the imaged pore–pore distances.

stricted to occupy only pore sites. Thus, a big part of the observed guest molecules did not perform a jump (≈80–90%). The great majority of the molecules that did jump moved to a nearest neighbor (NN) position (≈10%, red arrow). Some moved to the $\sqrt{3}$NN pore (≈1%, green arrow), and another ≈1% moved to the 2NN pore (blue arrow). However, we will argue later that most of the long jumps (>NN-distance) may be caused by two consecutive single jumps.

In order to obtain information about the hopping rates, one has to determine the probability $P_0(\tau)$ that a molecule does not move in the time interval τ it takes to record the STM image. Using the relation $P_0(\tau)=\exp(-h\tau)$, which results from Poisson statistics, allows the hopping rate h of the examined system to be calculated.[40–43] The number of observed molecules and τ then determine the statistical certainty of h. Because such a simplified approach does not account for multiple jumps, the resulting h will be systematically underestimated.[43]

Using this procedure, a pronounced difference in the hopping rates of C_{60} [$h(\theta=0.06)\approx 1\times10^{-3}$ s^{-1}] and C_{70} [$h(\theta=0.01)\approx 9\times10^{-2}$ s^{-1}] , where θ=coverage, has been found at the lowest measured guest molecule coverage. Since, under such dilute conditions, the lateral interfullerene interactions are minimal, these values approximately reflect the different jump barriers $E_a(\theta\approx0)$ for a single isolated guest molecule. A quantitative estimation of the diffusion barrier close to zero coverage can be obtained by using Equation (1):

$$h(\theta\approx 0)=\nu_0\exp\left(-\frac{E_a(\theta\approx 0)}{kT}\right) \quad (1)$$

where ν_o is the attempt frequency.[42,44,45] Assuming a standard value of $\nu_o=10^{13}$ s^{-1}, $E_a(\theta\approx0)$ was calculated to be 0.95±0.18 eV and 0.82±0.18 eV for C_{60} and C_{70}, respectively. The relatively large error is due to the uncertainty in the attempt frequency for which a lower limit of 10^{10} s^{-1} and an upper limit of 10^{16} s^{-1} was assumed.[42] Expecting the attempt frequency for both systems to be equal, the difference between the diffusions barriers of the two fullerenes $\Delta E_a(\theta\approx 0)$ can be calculated to be approximately 0.13±0.01 eV. These findings reflect the above-discussed differences in the host–guest interactions (manifested in the apparent heights) of the two types of fullerenes. Compared to C_{60}, C_{70} is obviously less effectively trapped within the porous framework; and, consequently, a lower activation energy for diffusion is found.

2.3. Jump Lengths

Since the determination of the hopping rates and the jump distances have been performed with a statistical ensemble of indistinguishable molecules, one can calculate the expected jump length λ with the help of h and the mean-squared displacement $\langle(\Delta x)^2\rangle$ using Equation (2):[43]

$$\langle(\Delta x)^2\rangle=\lambda^2 h\tau \quad (2)$$

Analysis of our data yielded values of $\lambda=4.5\pm0.3$ nm for C_{60} and $\lambda=4.2\pm0.2$ nm for C_{70}. These values correspond to 1.4±0.1 and 1.3±0.1 times the pore–pore distance of 3.3 nm, respectively. The jump length turned out to be independent of the fullerene coverage, to the extent to which λ could be determined in these experiments. These results clearly show that the present system is mainly ruled by single jumps, with a few contributions from long-jumps. In contrast to the distinct differences between the hopping rates of C_{60} and C_{70}, their jump lengths are indistinguishable.

2.4. Coverage-Dependent Hopping Rates

When increasing the fullerene coverage, the formation of short chains and islands of guest molecules can be observed, as shown in Figure 5.

Interestingly, for C_{70}, this behavior is already found at considerably low coverage ($\theta\approx0.1$); whereas, for C_{60}, it has only been observed at higher values ($\theta>0.5$). These findings clearly indicate a distinct interaction between the guest molecules that influences their mobility. Therefore, a systematic investigation of the hopping rates as a function of the fullerene coverage has been performed. Figures 6a and b show the hopping rates of the C_{60}–**1** and C_{70}–**1** assemblies as a function of the fullerene coverage.

One can clearly see that the two curves follow distinctly different trends that deviate considerably from the simple linear

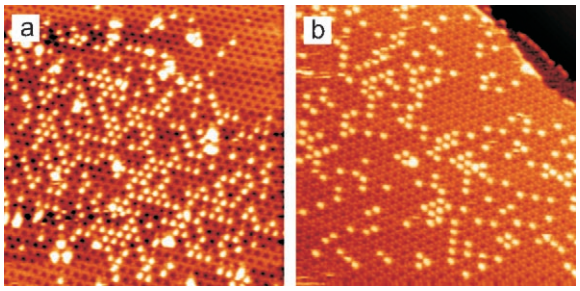

Figure 5. STM images of a) C_{60} (scan range: 100×100 nm^2, V_{bias} = 3.0 V, I_t = 9 pA, T = 298 K, θ = 0.4) and b) C_{70} (scan range: 100×100 nm^2, V_{bias} = 1.9 V, I_t = 24 pA, T = 298 K, θ = 0.2) on the porous porphyrin network at increased coverages. Note the pronounced formation of one-dimensional (1D) chains and 2D islands for both systems.

relation described below. The hopping rate of C_{60} increases between a coverage of zero and 0.3, followed by a strong decrease in the rate at higher values. In contrast, the hopping rate of C_{70} starts decreasing strongly right away, and rapidly reaches a value that is about two orders of magnitude lower. It should additionally be noted that annealing the samples to 400 K with subsequent cooling to 298 K did not significantly affect the guest molecule distributions or hopping rates. These findings clearly indicate that the investigated host–guest systems are in thermal equilibrium.

A semiquantitative interpretation of the coverage dependence can be done within the lattice gas or Bethe–Peierls approximation.[46] Adparticles (fullerenes in this case) are restricted to occupy only predefined sites (porphyrin pores here) on a rigid host lattice, and each of these adsorption sites is capable of hosting exactly one guest particle. Driven by thermal activation, particles are allowed to perform random jumps to neighboring positions of the lattice only if the target site is empty. This so-called site-blocking mechanism prevents the adsorption sites from double occupancy. The coverage dependence of the hopping rate within this approximation accordingly leads to $h(\theta) = h_0(1-\theta)$, when further neglecting any interparticle interactions (h_0 denotes the rate of a single particle in an infinitely diluted environment). The ––– in Figures 6a and b indicates this simplest model for the coverage dependence of the hopping rate. Obviously, the present systems are somewhat more complicated, since the formation of guest molecule chains and islands can be observed upon increasing the fullerene coverage (Figure 5). Such systems of interacting particles in a lattice gas have been addressed within the quasichemical approach.[26,46,47] In this approximation, the coverage-dependent hopping rate $h(\theta)$ can be analytically expressed by Equation (3):

$$h(\theta) = h_0 \frac{(1+\varepsilon)^{z-1}}{\left(1+\frac{\varepsilon}{f}\right)^z} \tag{3}$$

with [Eqs. (4)–(6)]:

$$\varepsilon = \frac{(\beta - 1 + 2\theta)f}{2(1-\theta)} \tag{4}$$

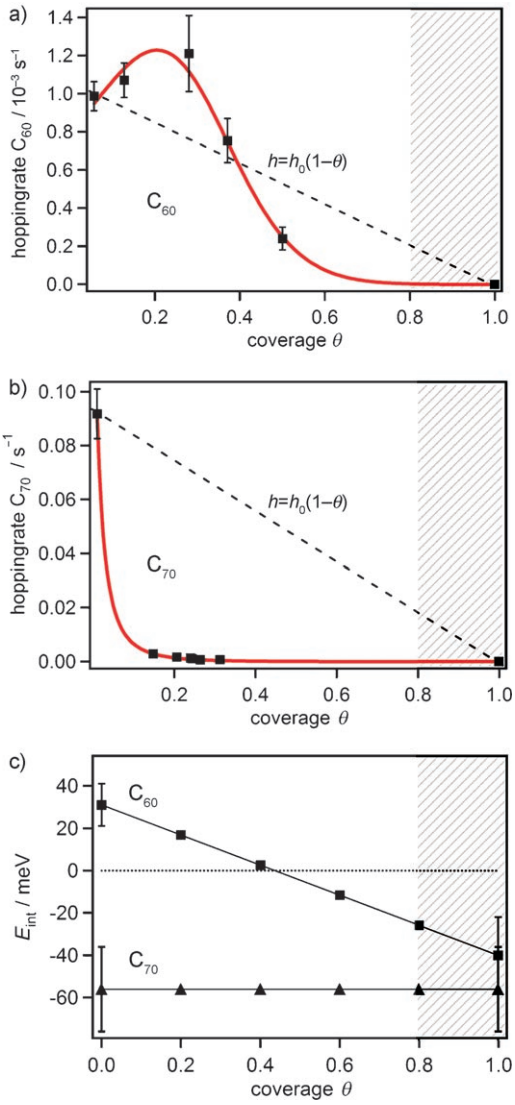

Figure 6. a) Coverage-dependent hopping rate of C_{60}. ■: data points as determined from the analysis of the STM data, with the uncertainty indicated by the error bars. The red line represents the best fit to the quasichemical approach. –––: linear dependence of the hopping rate as predicted by the lattice gas model with pure site blocking. The hatched area indicates coverages where the networks break down. b) Coverage-dependent hopping rate of the C_{70} molecules. c) Interaction energies of C_{60} and C_{70} as a function of coverage according to Equation (7) using the values given in Table 1.

$$\beta = \sqrt{1 - 4\theta(1-\theta)\left(1-\tfrac{1}{f}\right)} \tag{5}$$

$$f = \exp\left(\frac{E_{int}}{kT}\right) \tag{6}$$

where z, which is six in the case of an hexagonal lattice, is the coordination number. Furthermore, adparticles on the rigid lattice are supposed to interact with each other only through nearest-neighbor forces, characterized by the interaction energy E_{int} [Eq. (6)]. Each additional nearest-neighbor particle increases/reduces the binding energy of an adparticle by E_{int}, and therefore affects its jump probability. The parameter f in Equation (6) indicates the nature of the interaction: either at-

tracting for $f<1$ (which reduces the hopping rate) or repelling for $f>1$ (resulting in an increase of the adparticle mobility). However, this approach with constant interaction energy E_{int} does not necessarily match the behavior of real systems. In zeolites, for example, Krishna et al.[26] applied a linearly coverage-dependent interaction energy which accounts for the adparticle-induced modification of the lattice sites or cooperative guest effects, as described by Equation (7):

$$E_{int}(\theta) = E_0 + E'\theta \quad (7)$$

Here, E_0 is the interaction energy at zero coverage and E' is the slope of $E_{int}(\theta)$ as a function of coverage. Consequently, the experimentally derived hopping rates of the fullerene guest molecules on the porous porphyrin network have been fitted with Equations (3) and (7). The data point $h(\theta=1)=0$, which always exists in a lattice gas, has been enclosed in the data set in order to improve the quality of the fit. Nevertheless, it should be noted that around a coverage $\theta>0.8$, the complete porphyrin network collapses irreversibly for both fullerene structures. The solid lines in Figures 6a and b represent the fits to the experimental data; the values listed in Table 1 were obtained for the fitting parameters h_0, E_0, and E'. Figure 6c shows the trend of the interaction energy E_{int} explicitly as a function of coverage as calculated by Equation (7).

Table 1. Estimated energies present in the porphyrin–fullerene host–guest systems and the parameters for the quasichemical approach (QCA). The QCA parameters were obtained from Equations (3)–(7). The diffusion barriers and jump length were calculated using Equations (1) and (2), respectively.

		C_{60}	C_{70}
diffusion barrier	E_a [eV]	0.95 ± 0.18	0.82 ± 0.18
QCA parameters	h_0 [s^{-1}]	$7.9\pm0.7\times10^{-4}$	$1.3\pm0.2\times10^{-1}$
	E_0 [meV]	$+31\pm10$	-58 ± 20
	E' [meV]	-71 ± 18	≈0
jump length	λ [nm]	4.5 ± 0.3	4.2 ± 0.2

In order to compare the actual hopping rates with existing diffusion data, the self-diffusivity of the fullerenes may be estimated using Equation (8):[26,47,48]

$$D_{self}(\theta) = \tfrac{1}{4}h(\theta)\lambda^2 \quad (8)$$

For a given lattice, like in this case, this procedure is basically a multiplication with a constant, and therefore the qualitative trend of the hopping rates and self-diffusivity can be compared directly.

According to the quasichemical approximation, the pronounced decrease in the hopping rate of C_{70} is caused by the presence of a distinct attractive interaction between the nearest-neighbor molecules. This can be deduced from the negative value of $E_{int}=-58\pm20$ meV (Figure 6c). Within calculated error, the interaction energy has been found to be constant (i.e. $E'\approx0$) over the whole fullerene coverage range. It is worth noting that the value of E_{int} is comparable with that of Xe atoms on a Pt(111) surface at $T=80$ K, where a coverage-independent nearest-neighbor interaction energy $E_{int}\approx-10$ meV between the diffusing rare gas atoms was found using the same lattice gas model.[49]

In contrast, the situation with C_{60} is remarkably different. At low coverage, a repulsive nearest-neighbor interaction ($E_{int}>0$) is effective. E_{int} then decreases with increasing coverage and becomes attractive ($E_{int}<0$) above $\theta\approx0.45$, as shown in Figure 6c. Unlike in the case of C_{70}, it is not possible to fit the experimental data with a constant interaction parameter. Similar trends have also been reported in theoretical calculations of self-diffusivities in zeolites: as shown by Krishna et al.,[26] CH_4, Ar, or Ne in ITE-type zeolites at 298 K can be interpreted within the quasichemical approach using a linearly decreasing interaction energy [Eq. (7)]. These systems change their character from repulsive at low coverage to attractive in the high-loading regime, analogously to the system described here.

2.5. Pair Distribution

However, one should keep in mind that so far all results have been derived from a semi-empirical lattice gas model that is based on several severe simplifications. It is therefore worth double-checking the results obtained by this dynamic analysis with another independent method. This can be performed by analyzing the 2D pair distribution of the guest molecules on the porous network from static STM images. In contrast to the dynamic examination in Section 2.4, the pair distribution function reflects deviations of the observed guest molecule arrangement compared to a random particle distribution. Trost et al. explicitly derived the pair-distribution function $g(j)$ for particles adsorbed on discrete lattice sites, as expressed by Equation (9):

$$g(j) = (N\theta)^{-1}\sum_{i=1}^{N}\frac{n_i(j)}{m(j)} \quad (9)$$

where $n_i(j)$ is the number of particles around a particle i occupying the jth nearest-neighbor site.[50] The denominator $m(j)$ accounts for the totally available adsorption positions at the jth nearest-neighbor distance (Figure 4a). Normalization of the distribution is achieved by dividing by the coverage θ. Practically, deviations from $g=1$ indicate a divergence from the stochastic distribution, and thus imply the presence of an attractive or repulsive interparticle force for $g>1$ or $g<1$, respectively. The pair-distribution functions $g(j)$ for C_{60} (■) and C_{70} (▲), as shown in Figure 7, were derived from a positional analysis of several hundred fullerene molecules in different uniform STM images in the low coverage regime.

As can be seen from Figure 7, the pair-distribution functions of the two fullerenes clearly exhibit different trends. Whereas for C_{70} $g(1)=1.5$ indicates an attractive interaction, $g(1)=0.7$ for C_{60} shows the presence of repulsive forces between nearest-neighbor fullerenes. In the case of C_{70}, the distribution function stays slightly above unity at $j=2$, and then runs

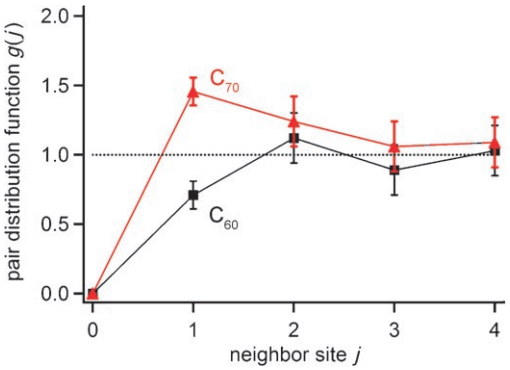

Figure 7. Pair distribution $g(j)$ as a function of neighbor site j for C_{60} (■) and C_{70} (▲) according to Equation (9) as obtained from several STM images ($\theta = 0.1$ for C_{60} and $\theta = 0.2$ for C_{70}). A definition for j is given in Figure 4a. Note, in particular, the pronounced difference between the two fullerenes at $j = 1$, which qualitatively reflects the result obtained within the quasichemical approach.

toward the average occupation probability for $j > 2$ (for C_{60} $g(j) \approx 1$ already for $j > 1$). As a result, both systems are predominately ruled by nearest-neighbor interactions, which show that, from this point of view, the quasichemical approach applied in Section 2.4 is appropriate.

From Boltzmann statistics, it is in principle possible to calculate the interparticle interaction energy from Equation (10):

$$g(j) = e^{-V_{\mathrm{eff}}(j)/kT} \qquad (10)$$

The interaction energy $V_{\mathrm{eff}}(j)$ is the so-called potential of mean force, which describes the interaction of a particle within an ensemble of other particles. Only in the limit of $\theta \rightarrow 0$ does this quantity equal the pair potential E_{int} used in Equation (6). At higher θ, contributions, for example, from entropic forces, have to be taken into account.[50] Therefore, the potential of mean force has been calculated only for low fullerene coverages, where a comparison with the pair potential is roughly acceptable. It follows from Equation (10) that $V_{\mathrm{eff}}(1) = +10 \pm 3$ meV for C_{60} (at $\theta = 0.1$) and $V_{\mathrm{eff}}(1) = -10 \pm 3$ meV for C_{70} (at $\theta = 0.2$). These values are comparable to the pair-interaction energies obtained from the quasichemical approach (Figure 6c), although they are lower by at least a factor of two to three. In particular, the opposite sign of the interfullerene interaction (attractive for C_{70} and repulsive for C_{60} at low coverage) predicted by the quasichemical approach is nicely reflected in the pair-distribution functions. The change of sign for the interaction energy of C_{60} at higher coverage ($\theta \geq 0.45$) reflects the formation of large fullerene islands, which are typically observed under such conditions as exemplarily shown in Figure 5a.

On the other hand, however, it should be noted that both the evaluation of the pair-distribution functions and the lattice gas analysis feature as an inherent disadvantage the fact that many-body interactions are completely ignored.[51] Therefore, the presented interguest interaction energies should be regarded as a first-order approximation.

2.6. Long-Range Interactions

From a mechanistic point of view, the observed long-range interguest interactions can only be mediated by either 1) the underlying silver substrate or 2) the porphyrin network. Direct through-space interactions can be ruled out because of the large fullerene–fullerene distance (≈ 3.3 nm), which excludes any significant van der Waals contributions, as recently reported.[30]

Long-range interactions that are mediated via electronic adsorbate–substrate coupling (case 1) have been observed for other molecular and atomic systems on surfaces.[52–57] Specifically, the local density of states (LDOS) at the Fermi energy has been found to spatially oscillate in the vicinity of adsorbates, resulting in the formation of standing electron waves with half the Fermi wavelength. For Ag(111), the periodicity of such standing waves around a perfectly scattering adsorbate would be 3.8 nm. For real adsorbates, for example, Ce atoms on Ag(111), this value reduces to 3.2 nm because of the imperfect scattering properties of the adsorbed metal atom.[56] These periodicities are close to the experimentally observed lateral pore–pore distance in the present porphyrin network. Furthermore, the small vertical distances, of only a few Angstroms of the fullerenes to the metal substrate, likely result in substrate–molecule charge transfer which has been reported on purely metallic substrates.[58] A contribution of the Ag substrate to the observed long-range interfullerene interaction is therefore possible, although no experimental evidence is available. This is due to the highly packed porphyrin layer, which completely decorates the Ag(111) surface and prevents the observation of standing wave oscillations in such a system.

Interactions mediated by the porous organic layer (case 2) have been identified in earlier investigations to be of importance by observations of conformational changes of the adsorbed porphyrins.[30,59] This type of interguest coupling is attributed to conformational and electronic modification (e.g. charge-transfer processes) of the porphyrin molecules upon adsorption of a fullerene guest. Local distortions in the porphyrin layer induced by a guest molecule are thus assumed to propagate through the porphyrin network, modifying the affinity of neighboring lattice sites to other adsorbates.

In the case of the adsorption of C_{70} within the present porous porphyrin network, the above-described mechanisms result in a decrease in the adsorption potential at the nearest-neighbor lattice sites around an initially filled pore, and thus in the stabilization of individual ad-C_{70}. According to the analysis within the quasichemical approach, each additional occupied neighboring pore reduces the interaction potential by a constant value. Overall, this results in a constant and negative pair-interaction energy E_{int} over the whole coverage range, as shown in Figure 6c. Consequently, the hopping rate of the C_{70} guest molecules decreases rapidly with increasing fullerene coverage, as expected for an ideal rigid host lattice.[26,46]

On the other hand, the situation is much more complicated for C_{60} guest molecules, since the interaction energy is dependent on the coverage, changing its sign from positive to negative with increasing coverage. These findings indicate that

the C_{60} guests strongly interact with the porphyrin host, and that this interaction is modified with increasing coverage. Such guest-induced modifications of porous networks are well-known from 2D and 3D porous networks, which can even be structurally transformed upon introduction or removal of guest molecules.[7–12,60] Thereby, physicochemical properties are significantly altered. Owing to the high flexibility of the porphyrin molecules in the present network, a similar mechanism is likely to be effective. This idea is further supported by the observation of bright–dim fluctuations of single porphyrin molecules that are propagating through the porous network, indicating conformational motion of the 3,5-di(*tert*-butyl)phenyl moieties (see Movie 1 in the Supporting Information).[30] Furthermore, the collapse of the porous porphyrin structure upon evaporation of additional guest molecules above the threshold of $\theta = 0.8$ is a clear sign of pronounced guest-induced host modifications.

From the experiments, however, it is not currently possible to identify the microscopic mechanisms behind the long-range interactions of both C_{60} and C_{70}. Most likely, a combination of the two proposed mechanisms is responsible for the observed behavior, with different contributions depending on the physical and chemical nature of the guest molecule.

3. Conclusions

The adsorption and the coverage-dependent mobility of C_{60} and C_{70} guest molecules in a nanoporous porphyrin host network have been investigated by means of STM. Single guest molecules were found to adsorb solely in the center of the porphyrin network pores. Time-lapse STM imaging series performed at 298 K further showed a distinct mobility of the fullerene guests, which displace from pore to pore, predominately via a single jump hopping mechanism. A detailed analysis of the coverage-dependent hopping rates within the quasichemical approach and the evaluation of pair-distribution functions additionally revealed pronounced differences in the long-range interguest interactions for the two investigated fullerenes. Besides metal substrate mediated coupling, the conformational flexibility of the porphyrin network likely plays a key role in this unique interaction between the fullerene guest molecules.

In general, such kinds of nanoscale host–guest systems are of special interest for future nanotechnological applications in catalysis, gas sorption, or in surface-supported chemistry, since the host networks selectively respond to different guest molecules and allow for the diffusion of the reacting species. A fundamental understanding of the mechanisms involved in transport and adsorption is therefore indispensable, and will contribute to a rational and effective engineering of future functional supramolecular nanoscale host–guest systems.

Experimental Section

All experiments were performed in a multichamber ultrahigh vacuum (UHV) system providing separate chambers for sample preparation and STM measurements. The base pressure in all chambers was approximately 2×10^{-10} mbar. Atomically clean and flat metal samples were prepared by repeated cycles of Ar^+-sputtering ($\approx$15 min) and thermal annealing ($\approx$ 870 K) on an Ag(111) single crystal substrate. Substrates prepared in such a way feature large areas with atomically flat terraces (up to 300 nm in width) separated by monoatomic steps, as evidenced by STM. The molecules used in this study, porphyrin **1**,[61] C_{60}, and C_{70}, are depicted in Figure 1a. Their chemical structures are drawn to the same scale, so as to reflect their respective sizes. The organic molecules were deposited by sublimation from a resistively heated tantalum crucible (Knudsen-cell-type evaporator). During evaporation, the substrate was kept at room temperature (298 K). The deposition rate was controlled by a quartz microbalance. Previous experiments have shown that the thickness of the molecular layer can be reproducibly controlled within an error of 10% with this setup. Deposition rates were of the order of 0.2 to 1.0 ML min^{-1} with an average chamber pressure rising up to 1×10^{-8} mbar, 2.5×10^{-9} mbar, and 1.5×10^{-9} mbar during the deposition of **1**, C_{60}, and C_{70}, respectively. The molecular arrangements on the substrate were studied by room-temperature STM. Chemically etched tungsten tips were heated by electron bombardment in situ before using them in the STM. All STM images were recorded in constant-current mode, using sample bias voltages of $\pm$2.0–3.0 V (tip held at ground potential) with a tunneling current of 10–50 pA. The typical scan speed was in the range of 200–600 nm s^{-1}. Imaging of all the molecular assemblies described herein was equally successful at positive and negative bias voltages. No differences were observed between the two polarities. Data acquisition was performed using a NANONIS^{TM} SPM Controller setup.

Van der Waals (vdW) volume and outer vdW surface of C_{70} were evaluated by means of the volume and surface functions as implemented in the MOE (Molecular Operating Environment) package (Chemical Computing Inc., Montreal, 2004) version 2004.03, starting from the C_{70} crystal structure coordinates.[37,38] The calculations were performed on an Intel Xeon 3.0 GHz biprocessor workstation. The corresponding vdW diameters were estimated by approximating C_{70} as a prolate spheroid. For the short and long axis of the fullerene, values of $d_{min} = 9.0 \pm 0.2$ and $d_{max} = 12.0 \pm 0.2$ Å were obtained.

Acknowledgements

We gratefully acknowledge the financial support of the Swiss National Science Foundation, the NCCR "Nanoscience", and the Swiss Federal Commission for Technology and Innovation, KTI. We also thank Nanonis Inc. for the fruitful collaboration on the data acquisition system and Luca Ramoino for numerous scientific discussions.

Keywords: diffusion · fullerenes · host–guest systems · porphyrins · supramolecular chemistry

[1] P. Bhyrappa, S. R. Wilson, K. S. Suslick, *J. Am. Chem. Soc.* **1997**, *119*, 8492.
[2] M. E. Davis, *Nature* **2002**, *417*, 813.
[3] F. Schüth, W. Schmidt, *Adv. Mater.* **2002**, *14*, 629.
[4] G. D. Fallon, M. A.-P. Lee, S. J. Langford, P. J. Nichols, *Org. Lett.* **2002**, *4*, 1895.
[5] G. M. Whitesides, B. Grzybowski, *Science* **2002**, *295*, 2418.
[6] D. W. Smithenry, S. R. Wilson, K. S. Suslick, *Inorg. Chem.* **2003**, *42*, 7719.
[7] S. Kitagawa, R. Kitaura, S. Noro, *Angew. Chem.* **2004**, *116*, 2388; *Angew. Chem. Int. Ed.* **2004**, *43*, 2334.
[8] K. Uemura, S. Kitagawa, K. Fukui, K. Saito, *J. Am. Chem. Soc.* **2004**, *126*, 3817.

[9] C. Mellot-Draznieks, C. Serre, S. Surblé, N. Audebrand, G. Ferey, *J. Am. Chem. Soc.* **2005**, *127*, 16273.
[10] S. Aitipamula, A. Nangia, *Chem. Eur. J.* **2005**, *11*, 6727.
[11] L. Dobrzanska, G. O. Lloyd, H. G. Raubenheimer, L. J. Barbour, *J. Am. Chem. Soc.* **2005**, *127*, 13134.
[12] J.-P. Zhang, Y.-Y. Lin, W.-X. Zhang, X.-M. Chen, *J. Am. Chem. Soc.* **2005**, *127*, 14162.
[13] S. Griessl, M. Lackinger, M. Edelwirth, M. Hietschold, W. M. Heckl, *Single Mol.* **2002**, *3*, 25.
[14] E. Mena-Osteritz, P. Bäuerle, *Adv. Mater.* **2006**, *18*, 447.
[15] G. B. Pan, J. M. Liu, H. M. Zhang, L. J. Wan, Q. Y. Zheng, C. L. Bai, *Angew. Chem.* **2003**, *115*, 2853; *Angew. Chem. Int. Ed.* **2003**, *42*, 2747.
[16] J. A. Theobald, N. S. Oxtoby, N. R. Champness, P. H. Beton, T. J. S. Dennis, *Langmuir* **2005**, *21*, 2038.
[17] S. Stepanow, M. Lingenfelder, A. Dmitriev, H. Spillmann, E. Delvigne, N. Lin, X. B. Deng, C. Z. Cai, J. V. Barth, K. Kern, *Nat. Mater.* **2004**, *3*, 229.
[18] M. Corso, W. Auwarter, M. Muntwiler, A. Tamai, T. Greber, J. Osterwalder, *Science* **2004**, *303*, 217.
[19] J. A. Theobald, N. S. Oxtoby, M. A. Phillips, N. R. Champness, P. H. Beton, *Nature* **2003**, *424*, 1029.
[20] S. J. H. Griessl, M. Lackinger, F. Jamitzky, T. Markert, M. Hietschold, W. M. Heckl, *J. Phys. Chem. B* **2004**, *108*, 11556.
[21] P. Demontis, G. B. Suffritti, *J. Phys. Chem. B* **1997**, *101*, 5789.
[22] C. Saravanan, F. Jousse, S. M. Auerbach, *Phys. Rev. Lett.* **1998**, *80*, 5754.
[23] H. Jobic, A. N. Fitch, J. Combet, *J. Phys. Chem. B* **2000**, *104*, 8491.
[24] A. I. Skoulidas, D. S. Sholl, *J. Phys. Chem. A* **2003**, *107*, 10132.
[25] A. I. Skoulidas, D. S. Sholl, R. Krishna, *Langmuir* **2003**, *19*, 7977.
[26] R. Krishna, D. Paschek, R. Baur, *Microporous Mesoporous Mater.* **2004**, *76*, 233.
[27] D. Dubbeldam, E. Beerdsen, T. J. H. Vlugt, B. Smit, *J. Chem. Phys.* **2005**, *122*, 224712.
[28] H. Jobic, J. Kärger, C. Krause, S. Brandani, A. Gunadi, A. Methivier, G. Ehlers, B. Farago, W. Haeussler, D. M. Ruthven, *Adsorption S1* **2005**, *11*, 403.
[29] A. I. Skoulidas, D. S. Sholl, *J. Phys. Chem. B* **2005**, *109*, 15760.
[30] H. Spillmann, A. Kiebele, M. Stöhr, T. A. Jung, D. Bonifazi, F. Cheng, F. Diederich, *Adv. Mater.* **2006**, *18*, 275.
[31] N. Katsonis, A. Marchenko, D. Fichou, *Adv. Mater.* **2004**, *16*, 309.
[32] X. D. Wang, V. Y. Yurov, T. Hashizume, H. Shinohara, T. Sakurai, *Phys. Rev. B* **1994**, *49*, 14746.
[33] D. M. Cyr, B. Venkataraman, G. W. Flynn, A. Black, G. M. Whitesides, *J. Phys. Chem.* **1996**, *100*, 13747.
[34] H. Fukumura, D. L-i, H. Uji-i, S. Nishio, H. Sakai, A. Ohuchi, *ChemPhysChem* **2005**, *6*, 2383.
[35] H. B. Bürgi, E. Blanc, D. Schwarzenbach, S. Liu, Y. Lu, M. M. Kappes, J. A. Ibers, *Angew. Chem.* **1992**, *104*, 667; *Angew. Chem. Int. Ed.* **1992**, *31*, 640.
[36] K. Hedberg, L. Hedberg, D. S. Bethune, C. A. Brown, H. C. Dorn, R. D. Johnson, M. De Vries, *Science* **1991**, *254*, 410.
[37] M. J. Hardie, P. D. Godfrey, C. L. Raston, *Chem. Eur. J.* **1999**, *5*, 1828.
[38] H. B. Bürgi, P. Venugopalan, D. Schwarzenbach, F. Diederich, C. Thilgen, *Helv. Chim. Acta* **1993**, *76*, 2155.
[39] K. M. Kadish, R. S. Ruoff, *Fullerenes: Chemistry, Physics, and Technology*, JohnWiley and Sons, Inc., New York, **2000**.
[40] B. G. Briner, M. Doering, H. P. Rust, A. M. Bradshaw, *Science* **1997**, *278*, 257.
[41] B. G. Briner, M. Doering, H. P. Rust, A. M. Bradshaw, *Phys. Rev. Lett.* **1997**, *78*, 1516.
[42] J. V. Barth, *Surf. Sci. Rep.* **2000**, *40*, 75.
[43] M. Schunack, T. R. Linderoth, F. Rosei, E. Laegsgaard, I. Stensgaard, F. Besenbacher, *Phys. Rev. Lett.* **2002**, *88*, 156102.
[44] S. Berner, *PhD Thesis*, University of Basel, Switzerland, **2002**.
[45] A. Zangwill, *Physics at Surfaces*, Cambridge University Press, Cambridge, **1988**.
[46] D. A. Reed, G. Ehrlich, *Surf. Sci.* **1981**, *102*, 588.
[47] D. A. Reed, G. Ehrlich, *Surf. Sci.* **1981**, *105*, 603.
[48] R. Gomer, *Rep. Prog. Phys.* **1990**, *53*, 917.
[49] D. L. Meixner, S. M. George, *J. Chem. Phys.* **1993**, *98*, 9115.
[50] J. Trost, T. Zambelli, J. Wintterlin, G. Ertl, *Phys. Rev. B* **1996**, *54*, 17850.
[51] L. Österlund, M. O. Pedersen, I. Stensgaard, E. Laesgaard, F. Besenbacher, *Phys. Rev. Lett.* **1999**, *83*, 4812.
[52] S. Lukas, G. Witte, C. Wöll, *Phys. Rev. Lett.* **2002**, *88*, 028301.
[53] N. Knorr, H. Brune, M. Epple, A. Hirstein, M. A. Schneider, K. Kern, *Phys. Rev. B* **2002**, *65*, 115420.
[54] V. S. Stepanyuk, A. N. Baranov, D. V. Tsivlin, W. Hergert, P. Bruno, N. Knorr, M. A. Schneider, K. Kern, *Phys. Rev. B* **2003**, *68*, 205410.
[55] M. Ternes, C. Weber, M. Pivetta, F. Patthey, J. P. Pelz, T. Giamarchi, F. Mila, W.-D. Schneider, *Phys. Rev. Lett.* **2004**, *93*, 146805.
[56] F. Silly, M. Pivetta, M. Ternes, F. Patthey, J. P. Pelz, W.-D. Schneider, *Phys. Rev. Lett.* **2004**, *92*, 016101.
[57] E. C. H. Sykes, B. A. Mantooth, P. Han, Z. J. Donhauser, P. S. Weiss, *J. Am. Chem. Soc.* **2005**, *127*, 7255.
[58] L.-L. Wang, H.-P. Cheng, *Phys. Rev. B* **2004**, *69*, 165417.
[59] D. Bonifazi, H. Spillmann, A. Kiebele, M. de Wild, P. Seiler, F. Y. Cheng, H. J. Guntherodt, T. Jung, F. Diederich, *Angew. Chem.* **2004**, *116*, 4863; *Angew. Chem. Int. Ed.* **2004**, *43*, 4759.
[60] D. X. Wu, K. Deng, Q. D. Zeng, C. Wang, *J. Phys. Chem. B* **2005**, *109*, 22296.
[61] D. Bonifazi, G. Accorsi, N. Armaroli, F. Song, A. Palkar, L. Echegoyen, M. Scholl, P. Seiler, B. Jaun, F. Diederich, *Helv. Chim. Acta* **2005**, *88*, 1839.

Received: March 28, 2006
Published online on June 21, 2006

